Passive Fractal Chipless RFID Tags Based on Cellular Automata for Security Applications

Mohammad N. Zaqumi [1], Jawad Yousaf [2], Mohamed Zarouan [1], Mohammed A. Hussaini [3], and Hatem Rmili [1,*]

[1] King Abdulaziz University, Department of Electrical and Computer Engineering, Jeddah 21589, Saudi Arabia
*hmrmili@kau.edu.sa

[2] Department of Electrical, Computer and Biomedical Engineering, Abu Dhabi University, United Arab Emirates
jawad.yousaf@adu.ac.ae

[3] Universiti Kuala Lumpur – British Malaysian Institute, Gombak 53100, Selangor, Malaysia

Abstract — In this paper, we propose a novel design of low-profile fractal chipless tags with unique specific electromagnetic responses. The tags are designed using cellular automata (Game of Life) technique to ensure the randomness of the generated fractal tags. The tags are simulated in CST Microwave Studio for the frequency range of 2 to 10 GHz. The tags are realized on FR4 substrate and their radar cross-section (RCS) characteristics are analyzed for the nine different tags for the three different polarizations (horizontal, vertical, and oblique). Each tag shows a unique signature resonance response. The obtained results of coding capacity (16-20 bits), coding spatial capacity (1-1.25 bits/cm^2), coding spectral capacity (2.15-2.9 bits/GHz), and coding density (0.15-0.18 bits/GHz x cm^2) of realized tags are very good. The presented tags could be used for the development of secure RFID systems.

Index Terms — Cellular automata, chipless RFID, fractal tags, game of life.

I. INTRODUCTION

Radiofrequency identification (RFID) tags are the backbone of the Internet of Things (IoT). These tags are also widely used in supply chain (inventory management, shipment tracking, etc.), biomedical, document security, and various civil and military applications [1-3]. Chipless RFID tags emerged as a low-cost solution because of their miniaturized size and no need for battery-powered components. The security of the data transfer has been a vital issue in RFID. Therefore, the exchange of information using RFID must be protected from hackers to ensure the safe usage of RFID in the aforementioned applications [4, 5].

Passive fractal chipless RFID tags have gained a lot of interest recently for wireless data transmission. Fractal tags exhibit interesting characteristics of multiband operation and broadband resonances in a limited size as well as good radiation characteristics, as compared to conventional non-fractal large size chipless tags [1, 6-8]. The broadband resonance characteristics in small size enhance the surface coding density of fractal tags.

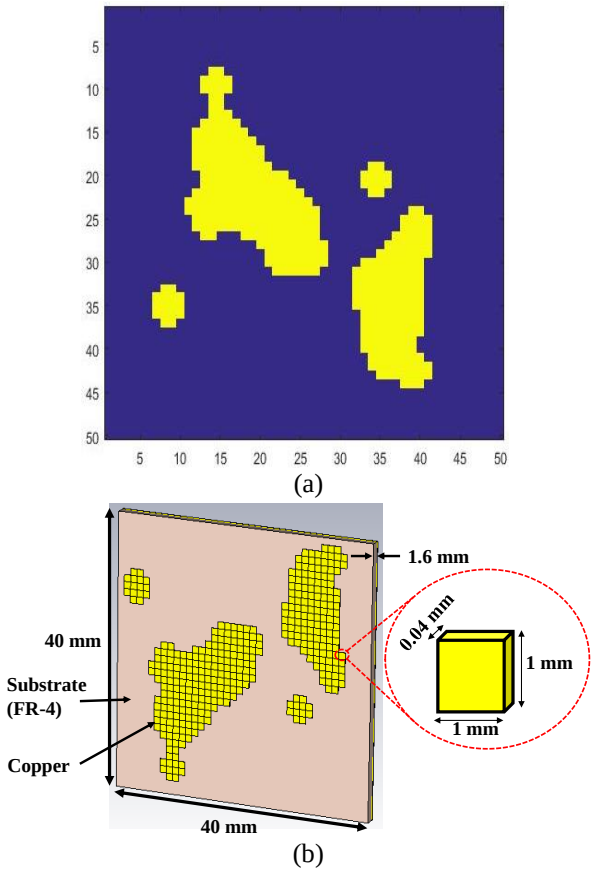

Fig. 1. (a) 2D form of game of life in Matlab; (b) CST structure of applied game of life on the chipless RFID tag.

Submitted On: April 4, 2021
Accepted On: May 16, 2021

https://doi.org/10.47037/2020.ACES.J.360510

The unique wideband resonance characteristics of irregular RFID tags which are used for the accurate detection of the tag, cannot be recognized by traditional readers. These interesting features of fractal tags make them a superior candidate for the security and safety applications such as authorized access control, counterfeiting, weapons recognition, passport system at airports, classified documents, currency notes, and cheques identifications; along with other wide range of conventional RFID applications [1, 2, 4-7].

For the non-fractal tags, the coding capacity (# of bits) and density are dependent on the number of the resonators in the tags. Although utilization of the bi-statics (dual polarization) measurements data and hybrid encoding procedure in the conventional (patch, split ring, slot, *etc*. [9-12]) resonators-based frequency domain (FD) tags could enhance their encoding capacities. However, for higher coding density, large size tags are required to increase the number of resonators in tags.

Many studies are available in the literature on the design of fractal RFID tags. Sultan implemented the polygon fractal loops for the UHF RFID applications [1]. Padmini *et al.* [7] presented the simulation-based design of Vicsek square fractal (square shape) passive tags. The findings of [7] suggested that the second iteration design of the Vicsek fractal provides better resonance characteristics for the detection of the designed tag. The authors in [8] used the micro-genetic algorithm (m-GA) for the shape optimization of the passive fractal RFID tags based on self-similar fractal line and patch. The Hilbert-curve fractal space-filling technique is used for the designing of the card-type dual-band loop tag for HF and UHF RFID applications in [9]. Rmili *et al.* [13] reported the fractal-jet fluid patch type chipless RFID-tag for security applications and suggested that encoding density of fractal tags can be enhanced by analyzing the both magnitude and phase of the reflection coefficient of the tag. Mouse *et al*. [14] proposed the simulation-based microstrip open resonator-based tags with two orthogonal fractal antennas for short-range RFID applications. The space-filling (Peano and Hilbert curved) based tags are reported in [15].

In this study, we propose a novel design of low-profile fractal chipless tags with specific electromagnetic responses that can be used for secure RFID systems. We investigate the design of new chipless tags based on the cellular automata (Game of Life) concept. We have considered a regular patch which we have modified by applying a sequence of programming procedures based on the cellular automata concept as illustrated in Fig. 1. The electromagnetic signature of RFID chipless tag and cellular automata geometries are usually self-similar and offer the possibility to increase the resonating length inside a limited area. We have obtained 100 tags with different structures of random square-shaped patches, which we have analyzed numerically by determining their radar cross-section (RCS) when illuminated with an incident electromagnetic wave within the range of 2-10 GHz. Computer Simulation Technology (CST) software was used for the numerical analysis of the tags. The selected designed structures out of 100 were then analyzed in terms of the capacity of coding by determining their coding density and RCS characteristics.

II. DESIGN OF TAGS USING CELLULAR AUTOMATA

A. Cellular automata and Game of Life (GoL)

The term cellular automata is plural and cellular automaton is its singular form. The concept was proposed by Stanislaw Ulam and John von Neumann in the 1940s [16]. The cellular automata is used in building a system of a large number of objects with varying states over time [17]. Cellular automata (cellular automaton singular) originates from automata theory in model computation, which is discrete [16]. A cellular automaton constitutes a grid of cells in which each cell exhibits a finite number of states (alive or dead). The states of each cell are changed, after defining its initial condition at time $t = 0$, depending on the characteristics of its neighboring cell through a set of rules [16].

The concept was evolved by Conway in the 1970s in terms of two-dimensional cellular automaton which was referred to as Game of Life (GoL) [18]. In GoL, the size of the neighborhood cells increases for the design of more random and complex applications. Initially, the Game of life appeared as an article in Scientific American in 1970 and soon has applied in the display of LEDs, screens, projection surfaces, and so on [18]. The main principles of the Game of life are directly related to simulation of the natural world with code such as creating a simulation that illustrates the characteristics and behaviors of biological systems of reproduction. Opposite to Von Neumann that generated an extremely complex system of states and rules, Conway wanted to get a similar “lifelike” result applying the simplest set of rules possible. The concept of Game of Life is applied in this study for the design of random fractal RFID tags.

B. Tag designs

Figure 1 shows the application of Game of life, which was firstly applied in Matlab as a 2D image. Figure 1 (a) shows a Matlab image of random cells in 2D form. The Matlab was linked to CST. Firstly, an application interface for CST-Matlab is required for applying the game of life. Once the game of life is

created as a 2D image in Matlab. Then the game of life will be executed in CST and the result will be as a 3D shape utilizing the API for CST-Matlab. The following notes are detailed steps for generating the game of life in the CST and Matlab.

- ❖ A full pack of an Application Interface (API) for CST-Matlab is available.
- ❖ Create/develop the game of life algorithm in Matlab.
- ❖ Generate/produce a 2D image of the game of life in Matlab.
- ❖ Create/develop the final sequence of code for chipless RFID tag and code for generation of the 2D image of the game of life in Matlab, then connect them with the CST in the presence of API for CST-Matlab.
- ❖ After the RFID tags are obtained in the CST thus perform simulation and further investigation in the CST for each generated tag.
- ❖ Select the best tags regarding their coding capacity or coding density.

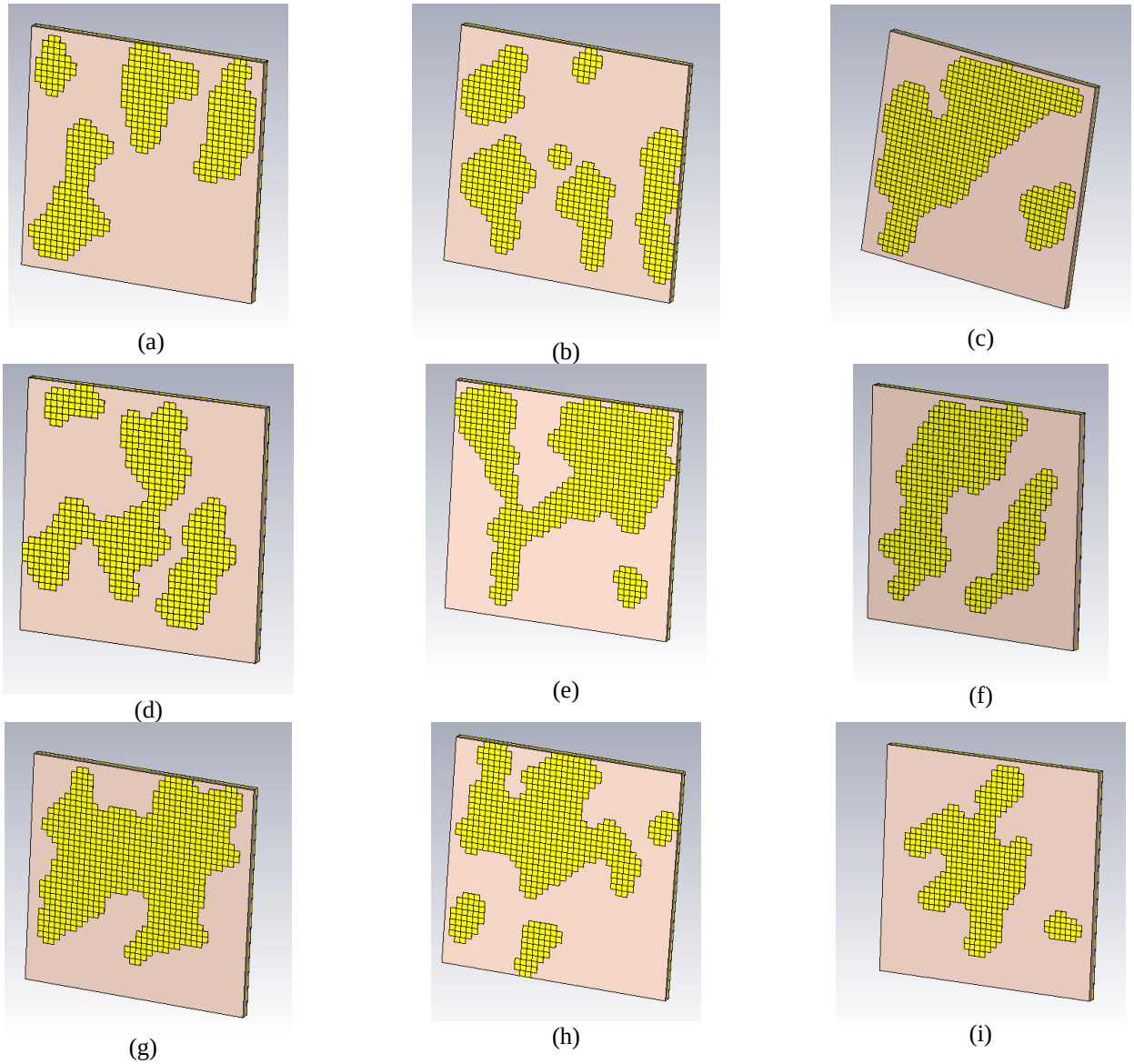

Fig. 2. CST structure of applied Game of life on the Chipless RFID tags: (a) Tag 1; (b) Tag 2; (c) Tag 3; (d) Tag 4; (e) Tag 5; (f) Tag 6; (g) Tag 7; (h) Tag 8; (i) Tag 9.

Figure 1 (b) illustrates the implementation of Game of life on the tag in CST. Each tag cell has dimensions of 1 mm x 1 mm with a thickness of 0.04 mm. The random shape of the metallic copper tag is etched on an FR4 substrate having a thickness of 1.6 m. The dimensions of the used FR4 substrate are 40 mm x 40 mm x 1.6 mm. The dimensions of all parameters of the realized tags are depicted in Table 1.

The geometries of the studied tags are illustrated in Fig. 2. The first structure (Fig. 2 (a)) is obtained next to the first iteration where the game of life is applied to the main structure. Additionally, the second, third, and fourth structure is obtained using the game of life from cellular automata. By repeating the same procedure, we obtain more structures with randomly shaped RFID tags utilizing the game of life as shown in Fig. 2. One hundred (100) such structures were realized and simulated in CST MWS. However, only a few structures of Fig. 2 are discussed here which shows good performance in terms of sensitivity and higher coding density as compared to other structures.

Table 1: Dimension of the realized tags

Parameter	Dimension
Substrate Dimensions	40 mm x 40 mm
Substrate thickness	1.6 mm
Substrate Dielectric constant	4.3 [F/m]
Conductor thickness	0.04 mm

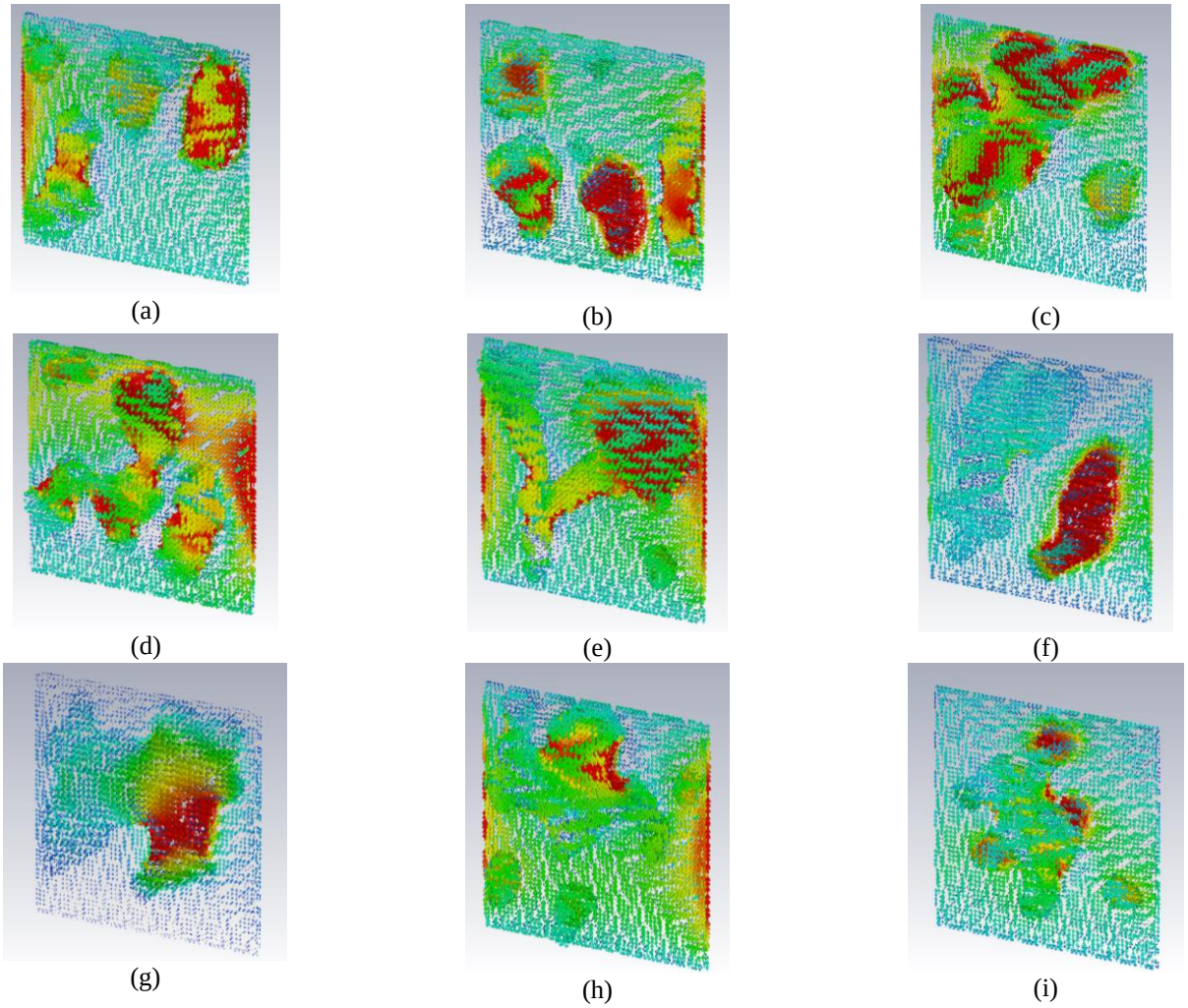

Fig. 3. Surface current distribution of realzied Chipless RFID tags in vertical polarization: (a) Tag 1 at f = 3.79 GHz, J_{max} = 0.219 A/m; (b) Tag 2 at f = 4.09 GHz, J_{max} = 0.258 A/m; (c) Tag 3 at f = 5.84 GHz, J_{max} = 0.134 A/m; (d) Tag 4 at f = 5.07 GHz, J_{max} = 0.162 A/m ; (e) Tag 5 at f = 3.42 GHz, J_{max} = 0.205 A/m; (f) Tag 6 at f = 2.72 GHz, J_{max} = 0.299 A/m; (g) Tag 7 at f = 2.25 GHz, J_{max} = 0.275 A/m; (h) Tag 8 at f = 3.34 GHz, J_{max} = 0.241 A/m; (i) Tag 9 at f = 7.9 GHz, J_{max} = 0.093 A/m.

The passive chipless RFID tag is excited with plane waves which induce the particular surface current distribution on the tag according to its structure. The analysis is performed for the frequency range of 2 to 10 GHz. The detection procedure of the passive chipless RFID tag is based on the analysis of the unique signature resonances in the received broadband backscattered signal from the designed tag at the RFID reader [7-9]. The presence of a large number of multiband resonances in the reflected signal from the fractal tag geometries provides additional security features to these tags compared to conventional chipless RFID tags [1-4]. The RCS characteristics are numerically investigated for each tag for three different polarization of horizontal, vertical, and oblique respectively.

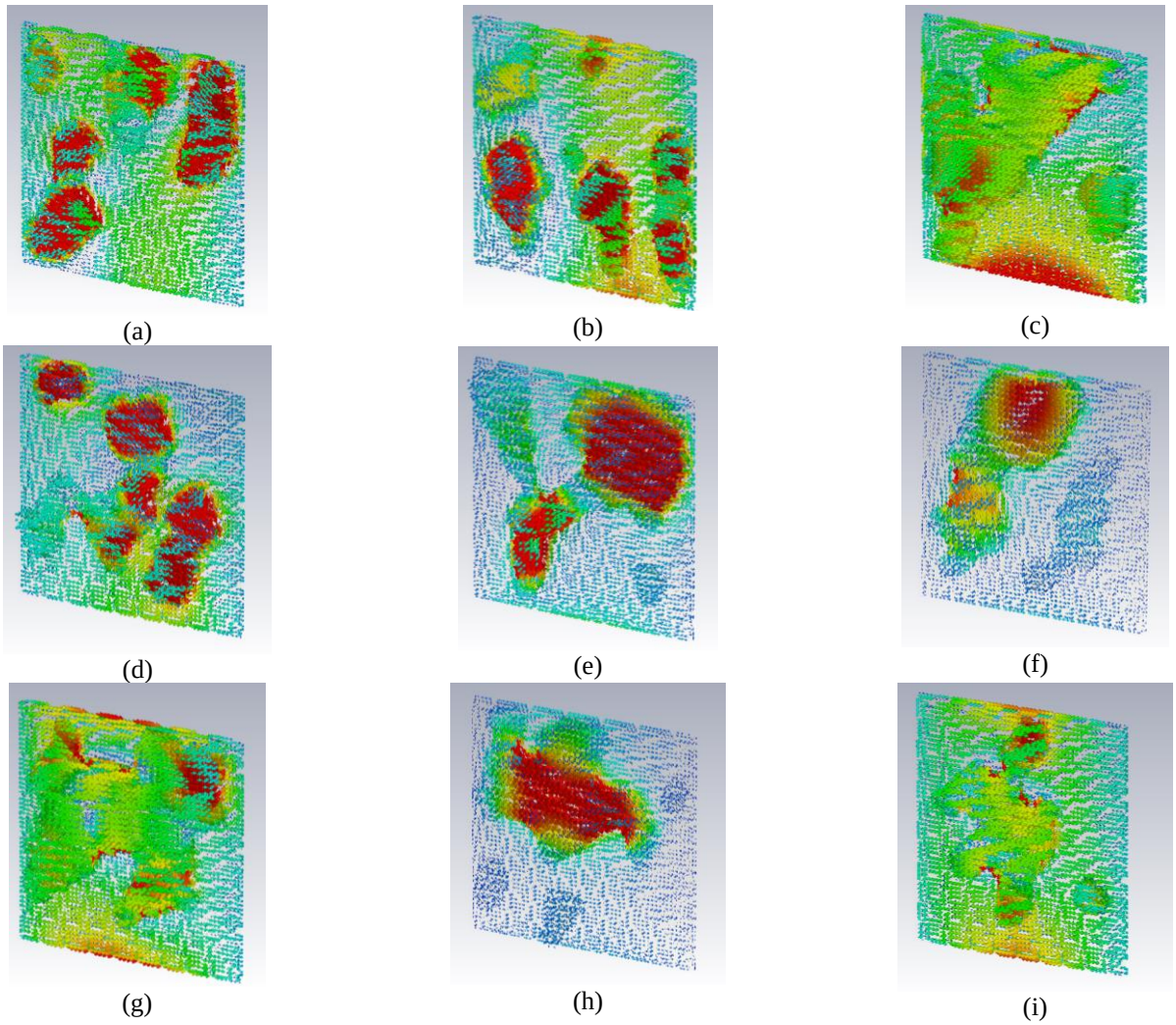

Fig. 4. Surface current distribution of realzied Chipless RFID tags in horizontal polarization: (a) Tag 1 at f = 7.26 GHz, J_{max} = 0.046 A/m; (b) Tag 2 at f = 5.79 GHz, J_{max} = 0.119 A/m; (c) Tag 3 at f = 3.94 GHz, J_{max} = 0.139 A/m; (d) Tag 4 at f = 6.03 GHz, J_{max} = 0.169 A/m; (e) Tag 5 f = 3.50 GHz, J_{max} = 0.157 A/m; (f) Tag 6 at f = 3.55 GHz, J_{max} = 0.127 A/m; (g) Tag 7 at f = 4.45 GHz, J_{max} = 0.118 A/m; (h) Tag 8 at f = 2.14 GHz, J_{max} = 0.234 A/m; (i) Tag 9 at f = 5.78 GHz, J_{max} = 0.046 A/m.

III. RESULTS AND DISCUSSION

A. Surface current distribution analysis

The surface current distributions of nine selected tags at their selected respective resonance frequencies in vertical polarization are depicted in Fig. 3. The distributions of Fig. 3 are obtained at the frequencies where the minimum RCS values were recorded for each tag. The current distribution results are plotted for the resonance frequencies of 3.79 GHz, 4.09 GHz, 5.84 GHz, 5.07 GHz, 3.42 GHz, 2.72 GHz, 2.25 GHz, 3.34 GHz, and 7.9 GHz for Tag 1, Tag 2, Tag 3, Tag 4, Tag 5, Tag 6, Tag 7, Tag 8, and Tag 9 respectively. Figures

4 and 5 illustrate the current distribution results in the horizontal and oblique polarizations. The obtained results of Figs. 4 and 5 are at their respective resonance frequencies in horizontal and oblique polarization for each tag.

The red color in Figs. 3, 4, and 5 graphs represent highly concentrated surface current areas. It shows the exciting parts of the tags at the selected frequencies. As can be noticed from Fig. 3 (a) that for Tag 1 the maximum value of surface current density at the resonance frequency of 3.79 GHz is 0.219 A/m (in the red portion) in vertical polarization. The maxim value of J_{max} for Tag 2 is 0.258 A/m which is obtained at the resonance frequency of 4.09 GHz. The metallic islands of the tags resonate at different frequencies depending on their size compared to the wavelength.

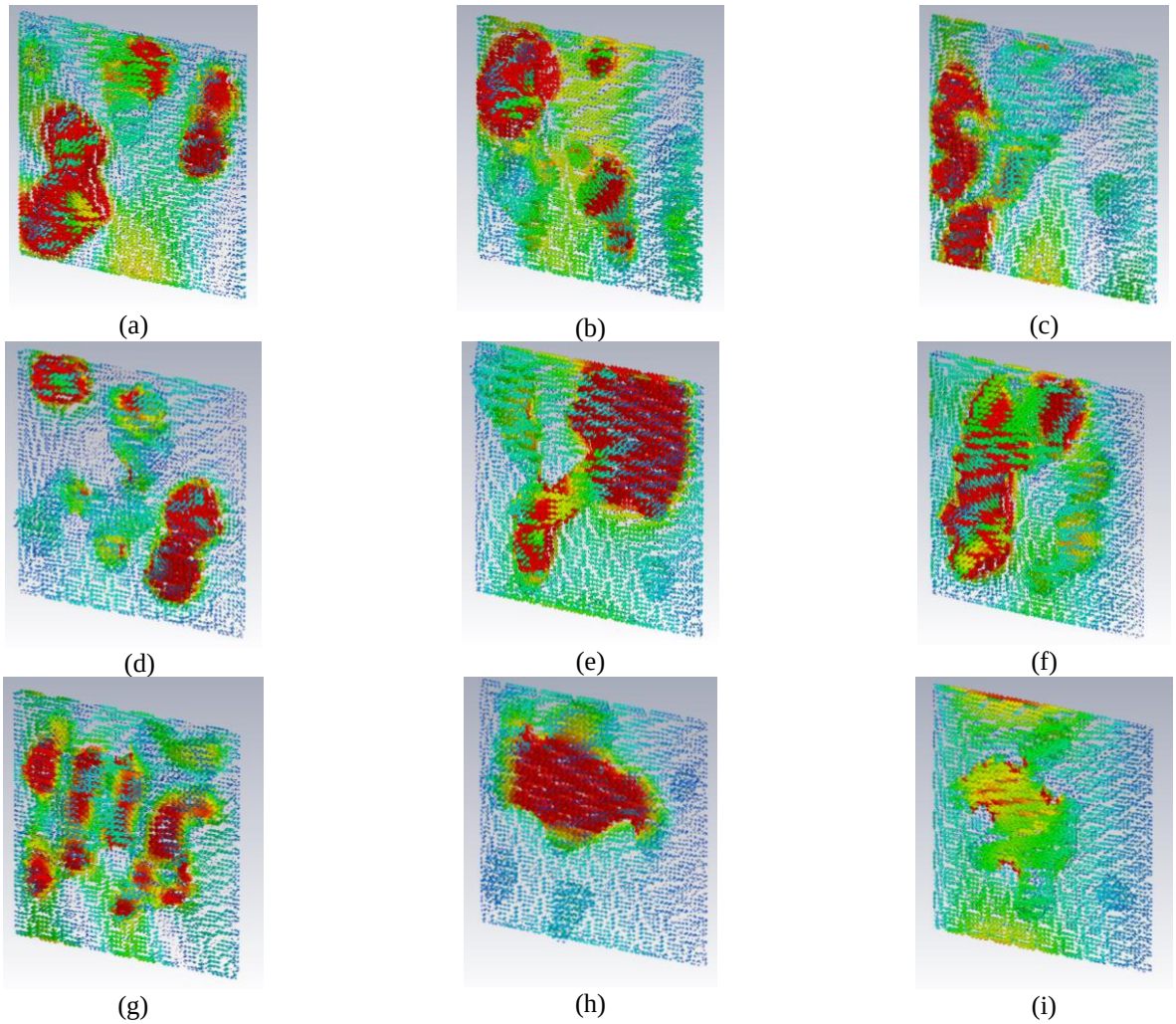

Fig. 5. Surface current distribution of realzied Chipless RFID tags in oblique polarization: (a) Tag 1 at f = 6.95 GHz, J_{max} = 0.066 A/m; (b) Tag 2 at f = 7.17 GHz, J_{max} = 0.087 A/m; (c) Tag 3 at f = 9.89 GHz, J_{max} = 0.051 A/m; (d) Tag 4 at f = 6.66 GHz, J_{max} = 0.131 A/m; (e) Tag 5 f = 3.54 GHz, J_{max} = 0.109 A/m; (f) Tag 6 at f = 5.67 GHz, J_{max} = 0.137 A/m; (g) Tag 7 at f = 9.69 GHz, J_{max} = 0.046 A/m; (h) Tag 8 at f = 2.14 GHz, J_{max} = 0.173 A/m; (i) Tag 9 at f = 3.86 GHz, J_{max} = 0.149 A/m.

The tags resonance frequency changes with the change in the polarization to horizontal and oblique. This can be noticed from the current distribution's maps of Figs. 4 and 5 for each tag. Tag 1 resonance frequency changes to 7.26 GHz and 6.95 GHz in horizontal and oblique polarization respectively. This changes the spreading of current around the metallic parts of the tag as can be noticed from Figs. 4 (a) and 5 (a) respectively for Tag 1. The current distribution of Tag 1 in horizontal and oblique polarization is quite different than its distribution in vertical polarization. Similar observations can be made for the Tags 2-9 by comparing their current distributions from Figs. 3-5 respectively.

This change in the current distribution depending on the fractal irregular shape of tags produce different unique RCS characteristics of each tag in each analyzed polarization.

B. RCS analysis

Figure 6 shows the RCS results of the nine realized tags for horizontal, vertical, and oblique polarizations. For Tag 1 from Fig. 6 (a), the resonant frequencies dips can be noticed at 4.25 GHz, 5.6 GHz, 5.84 GHz, 6.86 GHz, 7.26 GHz, and 8.67 GHz in horizontal polarization, at 2.98 GHz, 3.79 GHz, 4.27 GHz, 7.62 GHz, and 9.11 GHz in vertical polarization, and at 3.26 GHz, 4.24 GHz, 6.22 GHz, 6.95 GHz, 8.95 GHz, 9.09 GHz, and 9.58 GHz in oblique polarization respectively. Similar observations can be made for other realized tags in Fig. 2.

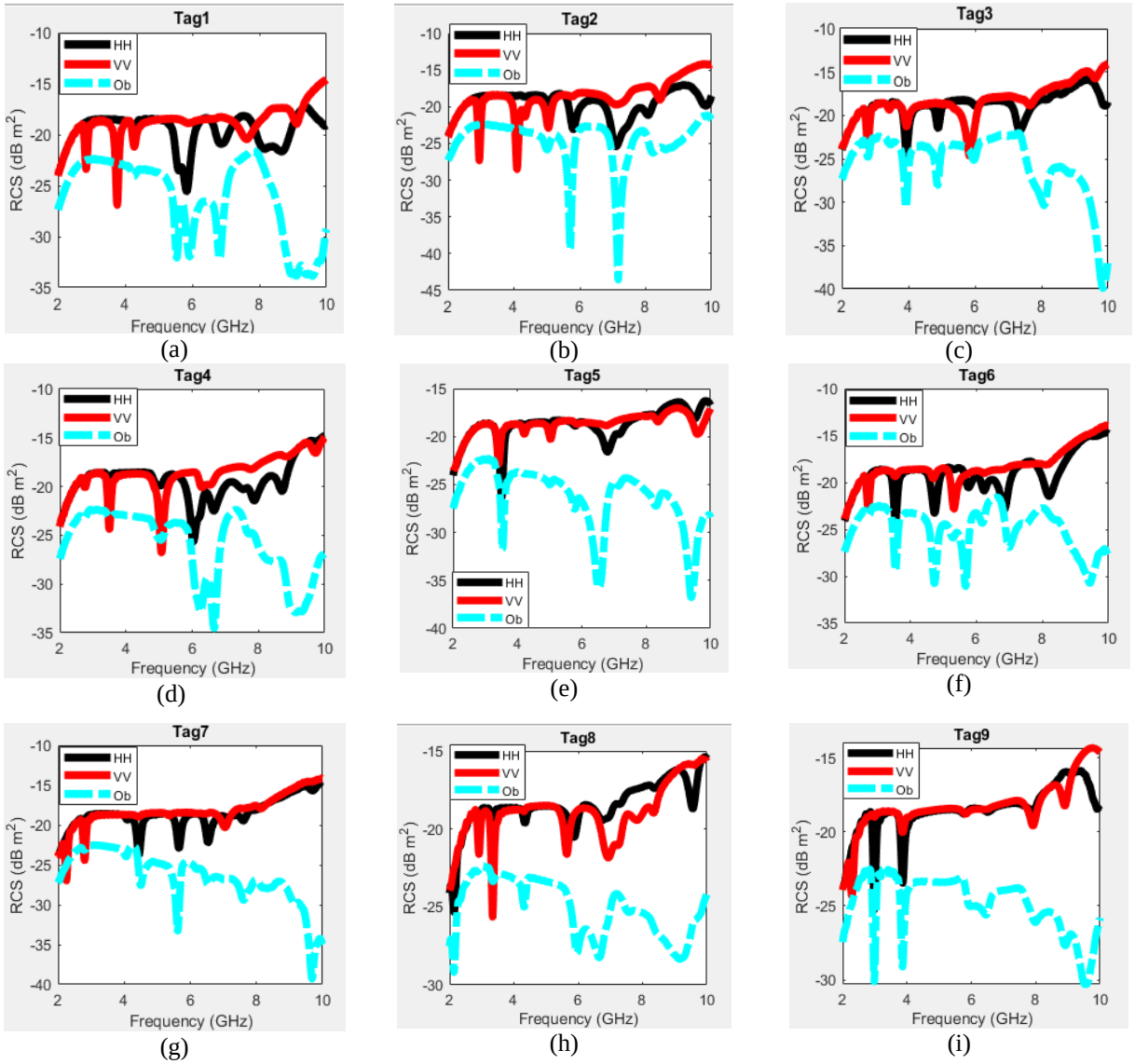

Fig. 6. RCS results of realzied Chipless RFID tags: (a) Tag 1; (b) Tag 2; (c) Tag 3; (d) Tag 4; (e) Tag 5; (f) Tag 6; (g) Tag 7; (h) Tag 8; (i) Tag 9.

Table 2 summarizes all resonance frequencies of all investigated tags of Fig. 2. We observe that each tag has its unique resonance characteristics in all three polarizations. The number of horizontal, vertical, and oblique polarization resonant frequencies changes for each realized tag. These resonance characteristics represent the different signatures of each fractal tag which can be used for its identification. The change in the fractal geometry of the tags due to the applied game of life concept ensures the randomness of the tags. This

results in unique current distribution on the metallic structure of the tag for the incident plane wave as can be noticed in Figs. 3, 4, and 5. Thus, a unique signature resonance response of each tag is obtained as can be observed from the signature resonance frequencies of each Tag in Table 2.

Table 3 compares the performance of analyzed tags in terms of the overall operating frequency range, coding capacity (bits), coding spatial capacity (bits/cm^2), coding spectral capacity (bits /GHz), and coding density (bits/GHz x cm^2). The overall operational frequency range of Tag 1 is 2.98 to 9.58 GHz (the range in which maximum resonance frequencies are recorded). There is a total of 18 resonance frequencies for these tags in three analyzed polarization which represent its 18-bit coding capacity. The observed coding spatial capacity, coding spectral capacity, and coding density for Tag 1 are 1.125 bits/ cm^2, 2.727 bits /GHz, and 0.17 bits/ GHz x cm^2 respectively. Similar observations can be made for other tags in Table 3. All investigated tags have a coding spatial capacity of more than 1 bit/cm^2 while the values of coding spectral capacity are greater than 2 bits/GHz for all tags. Among the analyzed tags, the highest coding spatial capacity (1.25 bits/cm^2) is recorded for Tags 4 and 8 respectively. The reason for these tags' superior performance is the availability of higher backscattered resonance frequencies from their randomized metallic structure based on GOL as compared to other tags. Tag 4 also outperforms all other tags in terms of coding spectral capacity (2.861 bits/GHz) and coding density (0.178 bit/GHz x cm^2). The summary of Table 3 reflects that the overall performance of the presented tags is very good in terms of the analyzed critical parameters of Table 3.

Table 2: Resonance frequency in (GHz) of characteristics of realized Chipless RFID tags of Fig. 2 and Fig. 6

	Polarization		
Tag #	**HH**	**VV**	**Oblique**
1	4.25, 5.6, 5.84, 6.86, 7.26, 8.67	2.98, 3.79, 4.27, 7.62, 9.11	3.26, 6.22, 6.95, 4.24, 8.95, 9.09, 9.58
2	5.79, 5.05, 7.11, 9.85, 8.07	2.95, 4.09, 4.33, 5.05, 7.11, 8.44	5, 5.71, 7.17, 8.22
3	2.77, 3.94, 3.42, 4.89, 6.03, 7.34, 9.88	2.78, 3.43, 3.94, 5.84, 7.65, 9.624	2.78, 3.92, 4.87, 5.99, 8.08, 9.89
4	2.76, 3.49, 5.03, 6.03, 6.65, 7.88, 8.70	2.76, 3.50, 5.07, 6.29, 7.76 8.84, 9.74	2.75, 3.50, 5.02, 6.26, 6.66, 9.14
5	3.50, 5.78, 6.78, 8.34, 9.51	3.42, 4.22, 5.03, 8.38, 9.61	3.54, 5, 5.78, 6.50, 7.14, 8.30, 9.39
6	2.71, 3.55, 4.73, 5.75, 6.23, 6.84, 8.19	2.72, 3.54, 4.70 5.33	2.74, 3.54, 4.72, 5.67, 5.29 6.18, 6.97, 9.44
7	2.78, 4.45, 5.67, 6.54, 7.62, 9.69	2.25, 2.8, 7.05, 8.14	4.06, 4.50, 5.62, 6.53, 7.61, 9.69
8	2.14, 3.33, 4.34, 5.88, 6.75, 8.38, 9.57	2.92, 3.34, 4.32, 5.65, 6.93, 7.26, 7.84, 8.35	2.14, 3.34, 4.32, 5.97, 6.66, 9.17
9	2.99, 3.86, 5.78, 6.52, 7.89, 9.91	2.29, 2.99, 3.86, 5.8, 7.90, 8.89	2.98, 3.86, 5.95, 6.45, 7.96, 8.92, 9.54

Table 3: Comparison of different characteristics of the realized nine Tags

Tag #	**Frequency Range (GHz)**	**Coding Capacity (bits)**	**Coding Spatial Capacity (bits/cm^2)**	**Coding Spectral Capacity (bits/GHz)**	**Coding Density (bits/GHz x cm^2)**
1	2.98-9.58	18	1.125	2.727	0.17
2	2.95-9.58	16	1	2.413	0.15
3	2.77-9.89	19	1.188	2.668	0.166
4	2.75-9.74	20	1.25	2.861	0.178
5	3.42-9.51	17	1.063	2.791	0.174
6	2.71-9.44	19	1.188	2.823	0.176
7	2.25-9.69	16	1	2.15	0.134
8	2.14-9.57	20	1.25	2.691	0.168
9	2.29-9.54	19	1.188	2.620	0.164

The uniqueness of the presented tags is the random fractal structure of each obtained tag. This provides additional security features to the presented tags as their characteristics cannot be decoded using a conventional RFID scanner or readers.

IV. CONCLUSION

This study has presented a novel design of fractal chipless RFID tags which were realized using the cellular automata concept for the secure RFID systems. The results of nine tags, out of realized 100 tags, are discussed. The obtained results show the unique signature random EM characteristics of each realized tag, adding additional security features to the presented chipless tags. The presented tags show good results in terms of coding capacity (16-20 bits), coding spatial capacity (1-1.25 bits/cm^2), coding spectral capacity (2.15-2.9 bits /GHz), and coding density (0.15-0.18 bits/GHz x cm^2). The presented tags could be used for potential applications in document security, bank cheques along other applications in IoT devices.

ACKNOWLEDGMENT

This project was funded by the Deanship of Scientific Research (DSR), King Abdulaziz University, under Grant No. (RG-39-135-40). The authors gratefully acknowledge technical and financial support of KAU.

REFERENCES

[1] Q. H. Sultan and A. M. Sabaawi, "Design and implementation of improved fractal loop antennas for passive UHF RFID tags based on expanding the enclosed area," *Progress In Electromagnetics Research C*, vol. 111, pp. 135-145, 2021.

[2] M. Borgese, S. Genovesi, G. Manara, and F. Costa, "Radar cross section of chipless RFID tags and BER performance," *IEEE Transactions on Antennas and Propagation*, vol. 69, no. 5, pp. 2877-2886, 2021.

[3] A. Ramos, Z. Ali, A. Vena, M. Garbati, and E. Perret, "Single-layer, flexible, and depolarizing chipless RFID tags," *IEEE Access*, vol. 8, pp. 72929-72941, 2020.

[4] V. Mulloni and M. Donelli, "Chipless RFID sensors for the internet of things: Challenges and opportunities," *Sensors*, vol. 20, no. 7, p. 2135, 2020.

[5] D. Dobrykh, I. Yusupov, S. Krasikov, A. Mikhailovskaya, D. Shakirova, A. Bogdanov, A. Slobozhanyuk, D. Filonov, and P. Ginzburg, "Long-range miniaturized ceramic RFID tags," *IEEE Transactions on Antennas and Propagation*, pp. 1-1, 2020.

[6] H. Rmili, D. Oueslati, I. B. Trad, J. M. Floch, A. Dobaie, and R. Mittra, "Investigation of a random-fractal antenna based on a natural tree-leaf geometry," *Inter. J. of Ant. and Propag.*, vol. 2017, p. 7, Art. no. 2084835, 2017.

[7] E. Pazmiño, J. Vásquez, J. Rosero, and D. Pozo, "Passive chipless RFID tag using fractals: A design based simulation," in *2017 IEEE Second Ecuador Technical Chapters Meeting (ETCM)*, pp. 1-4, 2017.

[8] Y. Watanabe, H. J. I. J. o. A. E. Igarashi, and Mechanics, "Shape optimization of chipless RFID tags comprising fractal structures," vol. 52, no. 1-2, pp. 609-616, 2016.

[9] M. Alibakhshi-Kenari, M. Naser-Moghadasi, R. A. Sadeghzadeh, B. S. Virdee, and E. Limiti, "Dual-band RFID tag antenna based on the Hilbert-curve fractal for HF and UHF applications," *IET Circuits, Devices & Systems*, vol. 10, no. 2, pp. 140-146, 2016.

[10] H. Huang and L. Su, "A compact dual-polarized chipless RFID tag by using nested concentric square loops," *IEEE Antennas and Wireless Propagation Letters*, vol. 16, pp. 1036-1039, 2017.

[11] D. Girbau, J. Lorenzo, A. Lazaro, C. Ferrater, and R. Villarino, "Frequency-coded chipless RFID tag based on dual-band resonators," *IEEE Antennas and Wireless Propagation Letters*, vol. 11, pp. 126-128, 2012.

[12] A. Ferchichi, N. Sboui, A. Gharsallah, and H. Baudrand, "New antennas based on triangular patch as a solution for RFID application," *Applied Computational Electromagnetics Society Journal*, vol. 25, no. 3, pp. 199-205, 2010.

[13] H. Rmili, D. Oueslati, L. Ladhar, and M. Sheikh, "Design of a chipless RFID tags based on natural fractal geometries for security applications," *Microwave and Optical Technology Letters*, vol. 58, no. 1, pp. 75-82, 2016/01/01 2016.

[14] M. E. Mousa, H. H. Abdullah, and M. E. d. A. El-Soud, "Compact chipless RFID tag based on fractal antennas and multiple microstrip open stub resonators," in *2018 Prog. in Elect. Res. Symp. (PIERS-Toyama)*, pp. 1332-1338, 2018.

[15] J. McVay, A. Hoorfar, and N. Engheta, "Space-filling curve RFID tags," in *2006 IEEE Radio and Wireless Symposium*, pp. 199-202, 2006.

[16] B. Chopard and M. Droz, *Cellular Automata*. Springer, 1998.

[17] S. Wolfram, "Cellular automata as models of complexity," *Nature*, vol. 311, no. 5985, pp. 419-424, 1984.

[18] J. Conway, "The game of life," *Scientific American*, vol. 223, no. 4, p. 4, 1970.